# Dependence of ion hydration on the sign of the ion's charge

Alan Grossfield[a)]
*Department of Biochemistry and Molecular Biophysics, Washington University School of Medicine, St. Louis, Missouri 63110*

The solvation of simple ions in water is studied using molecular dynamics simulations with a polarizable force field. Previous simulations using this potential demonstrated that anions are more favorably solvated in water than cations. The present work is an attempt to explain this result by examining the effects of ions on the surrounding water structure, with particular focus on the first solvation shell and its interactions with the surrounding water. We conclude that while the first solvation shell surrounding cations is frustrated by competition between ion-water and water-water interactions, solvation of anions is compatible with good water-water interactions. © *2005 American Institute of Physics.* [DOI: 10.1063/1.1829036]

## I. INTRODUCTION

The solvation of ions is of great importance in biological and physical chemistry. In particular, understanding ion solvation is critical to elucidating the mechanism by which ion channels distinguish between different ionic species. Viewed simply, alkali and halide ions are perfectly symmetric spheres distinguished only by their charge, size, and polarizability. While these differences can be quite small, they underlie the remarkable selectivity of biological ion channels. For example, although $K^+$ and $Na^+$ differ in size by only a few tenths of an angstrom, potassium channels such as KcsA transport $K^+$ 10 000 times faster.[1,2] Moreover, the fluctuations in the KcsA selectivity filter are significantly larger than the size difference between the ions, so the differentiation is not accomplished by simple steric incompatibility between the ion and the protein.[3] Rather, it is the thermodynamics of solvation which dictates selectivity. The solvation of the sodium ion in the channel is not as favorable as solvation in bulk water, resulting in a free energy barrier which slows its transfer. Thus, in order to understand the molecular mechanism of ion selectivity, we must first understand ionic hydration.

Significant efforts have been made to explore the physical properties of hydrated ions using a variety of experimental techniques, including x-ray and neutron diffraction and scattering, nuclear magnetic resonance, and vibrational spectroscopy.[4,5] However, these experiments are complicated by a number of factors, one of the most important of which is the requirement for electroneutrality. Specifically, electroneutrality means that it is not possible to study a given ionic species in solution at equilibrium without including neutralizing counterions. Thus, while the solvation thermodynamics of a neutral salt can be measured directly, it is impossible experimentally to separate them into contributions from the individual anion and cation. Instead, an additional assumption must be introduced to perform this separation. For ex-

ample, one could choose a reference salt and make the assumption that the solvation free energies of the cation and anion are equal.[6–8] Once the solvation free energy for a single ionic species is known unambiguously, all of the others can be determined using the principle of additivity and the data for the thermodynamics of neutral salts. Alternatively, one could perform the separation by making assumptions about the solvation of $H_3O^+$ and $OH^-$ to establish the solvation free energy of the proton,[9] or by extrapolating bulk solvation free energies from thermodynamic data on small water-ion cluster.[10] Unfortunately, the single ion solvation values obtained by these separations are very sensitive to the assumptions used to make the separation. As a result, there is considerable controversy as to the true solvation thermodynamics of individual ionic species with different tabulations in the literature disagreeing by as much as 15 kcal/mol.[6,9–16]

Molecular dynamics computer calculations can potentially resolve many of these issues. In contrast to the experiments, simulations can treat a single ion in solvation without difficulty, and as such can be used to compute single ion thermodynamics unambiguously. Moreover, molecular dynamics simulations contain a wealth of structural information which can be used to characterize the results. However, in order to perform these simulations, one must first choose repulsion-dispersion parameters for the ions. This has most commonly been done by choosing parameters which reproduce single ion solvation free energies.[17–19] Unfortunately, this process is complicated by the inconsistencies in the literature tabulations of single ion thermodynamic values, as discussed above,[6,9,10] which introduces large uncertainties into the parametrization process. As a result, the various ionic parameter sets have very different thermodynamic and structural properties when used in solution.[11,20]

A better approach would be to parametrize using data which does not suffer from the ambiguities introduced by the requirement for electroneutrality. For example, *ab initio* calculations[21,22] and mass spectroscopy experiments[23] involving small water-ion clusters in the gas phase can provide the kind of detailed structural and thermodynamic information required for parametrization. However, standard force

---

[a)]Current address: Biomolecular Dynamics and Scalable Modeling, IBM T. J. Watson Research Center, 1101 Kitchawan Road, P.O. Box 218, Yorktown Heights, NY 10598. Telephone: 914-945-2978. Fax: 914 945-4105. Electronic mail: agrossf@us.ibm.com

fields use fixed partial charges and represent electronic polarization implicitly, which means that parameters chosen for the gas phase are not appropriate for liquid simulations. For example, the dipole moment for water in gas phase is 1.85 D, while in liquid it is greater than 2.6 D;[24] using a rigid nonpolarizable water model intended for the bulk to fit gas phase ion-water interactions would produce ion parameters which overestimate the effective size of the ion in liquid. Moreover, previous work demonstrated that ion-water dimers computed using a standard nonpolarizable water model and ion parameters intended to reproduce bulk solvation to overestimate both the effective size of the ion and the water-ion dimer interaction energy in gas phase.[11] By contrast, fitting ion parameters to the ion-water dimer using the polarizable AMOEBA (atomic multipole optimized energizers for biomolecular applications) force field produces single ion solvation free energies which, when summed, correctly reproduce the experimental free energies for neutral salts to within 1 kcal/mol in multiple solvents.[11] By contrast, simulations using other force fields do not reproduce the salt values, erring by at least 5 kcal/mol.

One of the oldest and simplest models for the free energy of solvation for an ion is the Born equation[25]

$$\Delta A = -\frac{q^2}{8\pi\epsilon_0 R}\left(1-\frac{1}{\epsilon}\right), \tag{1}$$

where $\Delta A$ is the free energy, $q$ is the charge, $R$ is the effective radius of the ion, and $\epsilon$ is the dielectric constant of the medium. This simple model makes several specific predictions regarding relative ionic solvation free energies: (i) smaller ions should have more favorable solvation free energies; (ii) the free energy to transfer an ion to a more polar phase should always be negative; and (iii) the sign of the ion's charge does not matter. Although many groups have suggested improvements to the Born equation[16,26–29] these basic predictions are intrinsic to continuum theory.

These predictions are not consistent with our previous results.[11] We found that $Cl^-$, though clearly larger than $K^+$, had an aqueous solvation free energy that was 12 kcal/mol more favorable. Moreover, $Cl^-$ is more favorably solvated in water ($\epsilon\approx 80$) than in formamide ($\epsilon\approx 110$). Several recent theoretical works have produced analogous results for aqueous solvation. For example, the favorable solvation of $Cl^-$ is also predicted by a recent extension to the Born equation which takes into account the contribution of favorable dispersion interactions.[30] Moreover, Hummer et al. performed a series of Monte Carlo simulations, where they found that the free energy to charge a van der Waals (vdW) sphere was approximately the size of a methane molecule to $\pm e$, with the anion being more favorably solvated by more than 40 kcal/mol.[31] The authors hypothesized that the overly favorable anion solvation is in part an artifact of the absence of a vdW term between the water hydrogens and the ions, which allows the hydrogens to pack very close to the anions. However, this is not the case for the results of Grossfield et al.,[11] since the AMOEBA water model includes repulsion-dispersion terms on water hydrogens.[32]

The present work will explain the solvation free energies of ions in water by examining their effects on solvent struc-

TABLE I. Parameters for ions. $R_{min}$ and $\epsilon$ are the parameters for the buffered 14-7 repulsion-dispersion potential, in angstrom and kcal/mol, respectively, and $\alpha$ is the polarizability in $Å^3$. The parameters for $Na^+$, $K^+$, and $Cl^-$ are identical to those used in the work by Grossfield et al. (Ref. 11).

| Ion | $R_{min}$ | $\epsilon$ | $\alpha$ |
|-----|-----------|------------|----------|
| $Na^+$ | 3.02 | 0.26 | 0.12 |
| $K^+$ | 3.71 | 0.35 | 0.78 |
| $Cl^-$ | 4.13 | 0.34 | 4.00 |
| $Br^-$ | 4.38 | 0.33 | 5.90 |

ture, using molecular dynamics simulations with the polarizable AMOEBA force field. By comparing the solvent structure around a series of cations, anions, and neutral particles, we will distinguish the effect of the ions' size and charge, and explain the observed deviations from the Born equation at a molecular level.

## II. METHODS

Molecular dynamics simulations were performed on systems consisting of a single ion and 216 water molecules embedded in a periodic cubic box 18.643 Å on a side. The AMOEBA force field was used for all calculations.[24,33] This potential uses a sophisticated electrostatics model involving permanent partial charges, dipoles, and quadrupoles on each atom, with electronic polarization represented via induced dipoles. Long range electrostatics are accounted for using Ewald summation,[33,34] with the real space cutoff set to 9 Å, the Ewald coefficient set to 0.42 $Å^{-1}$, and "tin-foil" boundary conditions. Repulsion-dispersion or vdW interactions are represented using a buffered 14-7 potential,[35] and were smoothly truncated at 12 Å. Previous work has shown that this force field accurately reproduces the properties of liquid water under both ambient conditions[24] and at extremes of temperature and pressure,[36] and is able to accurately predict the solvation free energies of neutral salts in multiple solvents.[11] The parameters for the water model are those given by Ren and Ponder,[24] while the ion parameters are shown in Table I.

The equations of motion were integrated using the Beeman variant of the velocity Verlet integrater, using a 1 fs time step.[37] Coordinates were saved every 0.1 ps. The temperature was set to 300 K using the Berendsen weak coupling method.[38] Induced dipoles were iterated until no dipole changed by more than 0.01 D upon successive iterations. Each simulation was run for 200 ps, with the first 50 ps discarded as equilibration. All simulations were run using version 3.9 of the TINKER simulation package, with local modifications.[39] Analysis was performed using various programs from the TINKER package or locally written programs and scripts.

Simulations were performed examining the solvation of four naturally occurring ionic species: $K^+$, $Na^+$, $Cl^-$, and $Br^-$. In addition, a second set of simulations was performed for $K^-$, $Na^-$, $Cl^+$, and $Br^+$; for these simulations, the charge on the ion was inverted, while the vdW and polarizability parameters were left unchanged. Similarly, two more sets of simulations were performed for these species with

TABLE II. Effective radii for the ions, measured as the distance to the first minimum of the ion-oxygen radial distribution function. "Positive" and "negative" refer to the ions with $+1e$ and $-1e$ charges. "Neutral" refers to the species with charge and polarizability set to zero, although the results for polarizable uncharged species were virtually identical.

| Ion | Positive | Negative | Neutral |
|---|---|---|---|
| Na | 3.3 | 3.1 | 5.0 |
| K | 3.6 | 3.6 | 5.1 |
| Cl | 3.9 | 4.0 | 5.3 |
| Br | 4.1 | 4.1 | 5.5 |

TABLE III. Coordination number for the ions, measured as the number of water oxygens within the effective radius, as defined in Table II. "Positive" and "negative" refer to the ions with $+1e$ and $-1e$ charges. The values marked with asterisks differ slightly from those reported in the work by Grossfield *et al.* (Ref. 11) because they were computed by direct analysis of the trajectories instead of summing the RDF. The difference between the reported $Cl^-$ values is due to an error in the previous work.

| Ion | Positive | Negative |
|---|---|---|
| Na | $5.9^* \pm 0.7$ | $4.6 \pm 0.6$ |
| K | $6.9^* \pm 1.0$ | $6.1 \pm 0.8$ |
| Cl | $8.6 \pm 1.4$ | $7.7^* \pm 1.3$ |
| Br | $9.0 \pm 1.5$ | $8.0 \pm 1.5$ |

their charges set to zero: one with the polarizability set the same as for the naturally occurring species and one with the polarizability set to zero.

The electrostatic potential at the neutral "ions" was estimated as

$$V = \frac{\langle U(q) - U(0) \rangle}{q}, \tag{2}$$

where $U(q)$ is the system's potential energy with a test charge $q$ placed on the ion. The potentials were computed with $q = 0.0001e$, although care was taken to verify that the same answer was obtained across a range of $q$ values, which means that $O(q^2)$ terms due to the Born self-energy, finite size corrections, and polarization due to the test charge could be safely neglected.[31,40–43]

When analyzing solvent structure, a water-water hydrogen bond was defined to be an interaction where the O–H distance was less than 2.8 Å, and the O–H–O angle was greater than 120°. This specific definition is reasonable but somewhat arbitrary, in that a different choice would slightly alter the number of hydrogen bonds we would find. This is not particularly important, as we are mostly concerned with variations in the hydrogen bonding patterns around different ionic species. The statistical uncertainty in the number of hydrogen bonds was computed using Monte Carlo bootstrap error analysis.[11,44] For a time series with $N$ data points, a bootstrap trial consisted of selecting $N$ points randomly from the time series, allowing duplication, and computing the average for that sample. We performed 1000 bootstrap trials and computed the statistical uncertainty as the standard deviation of the averages from the trials.

The lifetime of water structure in the first solvation shell was computed from the autocorrelation function of the instantaneous ionic coordination number. The coordination number was computed as the number of waters with oxygens within the effective ionic radius, which we defined to be the distance to the first minimum of the ion-O radial distribution function (see Tables II and III). We then computed the autocorrelation function of this time series as

$$C(\tau) = \frac{\langle (N_c(\tau) - \langle N_c \rangle)(N_c(0) - \langle N_c \rangle) \rangle}{\sigma(N_c)}, \tag{3}$$

where $N_c(t)$ is the coordination number for the ion at time $t$, $\sigma(N_c)$ is the variance, and angle brackets indicate the thermodynamic average. For all of the ions studied, the correlation function was not well described as a single exponential, but did fit well to a sum of two exponentials

$$C(t) = w_1 e^{-t/\tau_1} + w_2 e^{-t/\tau_2}. \tag{4}$$

At long time intervals, the correlation function became noisy due to poor sampling. To prevent this from influencing the fit, only the first 10 ps of the autocorrelation function was used. Because we only recorded coordinate sets every 0.1 ps, we cannot detect events occurring on a faster time scale. As a result, if a water molecule were to leave the first solvation shell and be replaced within 0.1 ps, the event would not be accounted for.

## III. RESULTS

### A. Solvent structure around ions

The primary theoretical tool for examining molecular structure in solution is the radial distribution function (RDF). Figure 1 shows the radial distribution functions for water
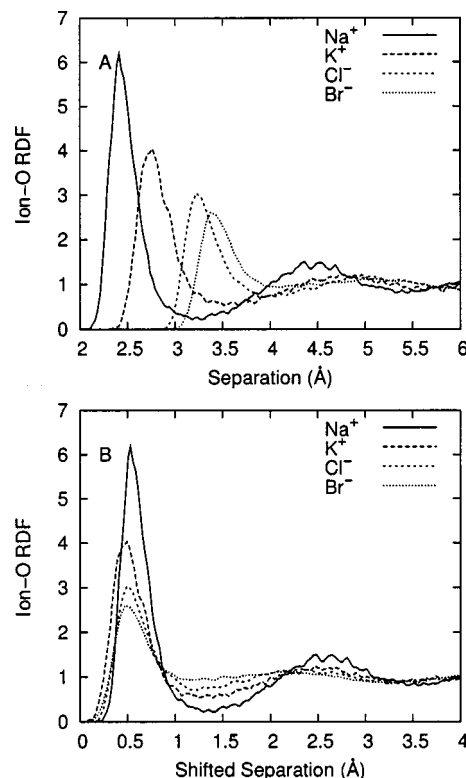


FIG. 1. Radial distribution functions for water oxygens around the ions. (a) The standard RDFs and (b) the RDFs shifted such that the first peaks overlap.
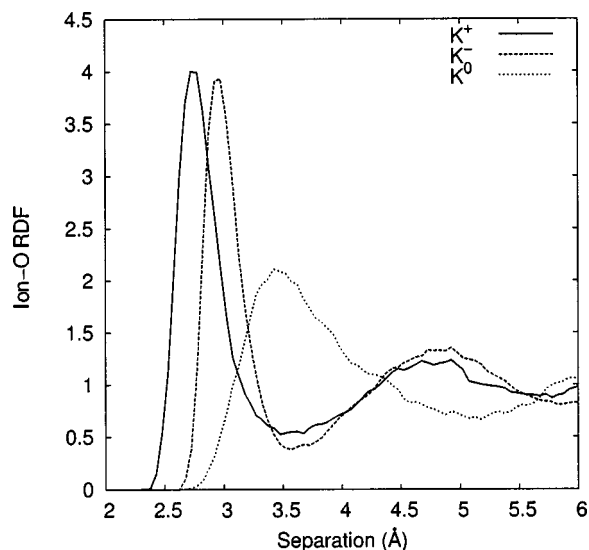
FIG. 2. Radial distribution functions for water oxygens around the potassium. K$^+$, K$^-$, and K$^0$ refer to the cationic, anionic, and neutral forms for potassium. The ions had the same vdW parameters in all three calculations. K$^-$ was assigned the same polarizability as K$^+$, while for K$^0$ the polarizability was 0 Å$^3$.

TABLE IV. The heights of the first peak and minimum for the ion-O radial distribution functions.

| | Positive | | Negative | | Neutral | |
| --- | --- | --- | --- | --- | --- | --- |
| Ion | Peak | Well | Peak | Well | Peak | Well |
| Na | 6.2 | 0.2 | 6.3 | 0.1 | 2.1 | 0.7 |
| K | 4.1 | 0.5 | 4.0 | 0.4 | 2.1 | 0.7 |
| Cl | 2.9 | 0.7 | 3.0 | 0.7 | 2.1 | 0.7 |
| Br | 2.6 | 0.8 | 2.7 | 0.9 | 2.1 | 0.7 |

oxygens around the naturally occurring ionic species. The results in Fig. 1(a) are completely as expected: as the ions get larger, the first peak moves outward and becomes less pronounced. In Fig. 1(b), the direct effects of ion size are removed from the plots by shifting the RDFs such that their first peaks are in the same position. We can see that the location of the first minimum and second peak relative to the first peak are largely unaffected by the ion size with the exception of Na$^+$, where both appear to be shifted slightly outward. Moreover, the larger the ion, the less structured the solvent appears to be, as evidenced by the decreased depths of the first minimum and height of the second peak. However, these data alone do not allow us to directly separate the effects of ionic size and charge on solvent structure because both variables are changed simultaneously.

We approach this problem by examining simulations of several unphysical ions, such as Na$^-$ and Cl$^+$, which we model by inverting the ionic charge while leaving the vdW and polarizability parameters unchanged. Although these ions do not represent realistic physical entities, the resulting calculations cleanly distinguish the effects of ionic size and charge.

With this in mind, Fig. 2 shows the distribution of water oxygens around potassium as a function of the ion's charge. The first peaks for K$^+$ and K$^-$ have virtually identical heights, with the latter shifted outward by roughly 0.2 Å. By contrast, the first minimum is in virtually the same place in both curves. The oxygen peak shifts because the water oxygen directly solvates the cation, while the anion is solvated by the water hydrogen. This may also account for the fact that the RDF about the anion appears slightly more structured, with a deeper first minimum and higher second peak.

The RDF for water around the nonpolarizable and uncharged K$^0$ is shown as well. It is qualitatively different from that of the two charged species; the first peak is much lower

and broader and is located much farther out. This is to be expected, since eliminating the charge allows unfavorable vdW interactions between the ion and the first solvation shell to relax. Moreover, the vdW interactions the neutral particles can make are not sufficiently favorable to compete with water-water hydrogen bonding interactions. The RDFs produced when K$^0$ was assigned the same polarizability as K$^+$ were indistinguishable from the nonpolarizable case (data not shown). Although Fig. 2 only shows the RDFs for potassium, the other elements behave similarly.

These results make it clear that the ion's charge can in principle have a significant effect on the its apparent size in solution. In estimating the ions' size, we choose to define the effective radius as the location of the first minimum of the ion-O RDF. Physically, this corresponds to including the first solvation shell around the ion in our definition of its size. Table II shows the effective radii for all of the ions simulated. For each of the four elements, the charged species have similar effective radii regardless of the charge sign, while the radii of the uncharged species are roughly 1.5 Å larger. This does not imply, however, that the solvent packing around the ions is independent of charge. Rather, the coordination number for the ions, computed as the average number of water oxygens located within the first solvation shell of the ion, varies dramatically with the ions' sign. Table III summarizes these results: for ions with identical vdW potentials, the cation is coordinated by roughly one more water molecule than the equivalent anion. The coordination numbers computed here are somewhat larger than those computed via quantum molecular dynamics and quasichemical theory.[45,46] However, the values produced by the two *ab initio* methods differ somewhat, and it is not entirely clear that the optimum coordination number as defined by quasichemical theory should be equal to that produced by analyzing the radial distribution function. The ion coordination number typically shows fluctuations of more than one water molecule, indicating that ion-coordination involves a number of different first shell conformations.

Table IV characterizes the ion-O RDFs for the various species in terms of the heights of the first peak and minimum. As before, when the ions get bigger, the degree of structure in the waters around them diminishes, demonstrated by the lower peak heights and higher minima. Again, the RDFs for each element do not appear to be particularly sensitive to the sign of the charge on the ion. This trend is not obeyed by the solvation of the neutral species, where the peak heights and well depths are constant. Indeed, if the RDFs for the neutral particles are shifted such that the loca-
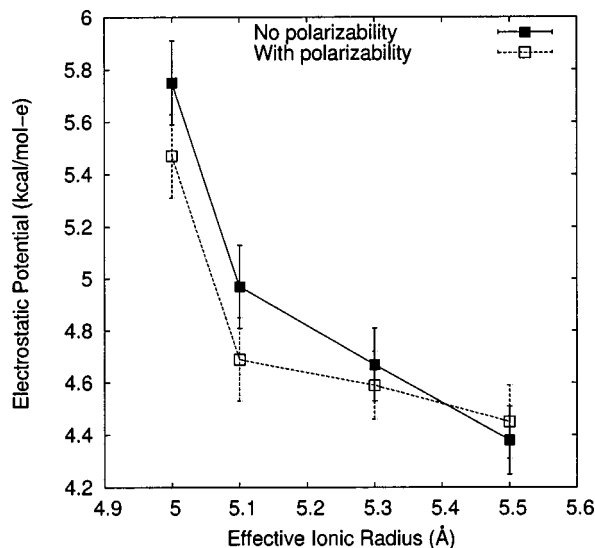
FIG. 3. Electrostatic potential at the center of the neutral ''ions,'' in kcal/mol-$e$, as a function of the effective ionic radii from Table II. Curves are shown for neutral species with and without polarizability. The error bars represent standard deviations.
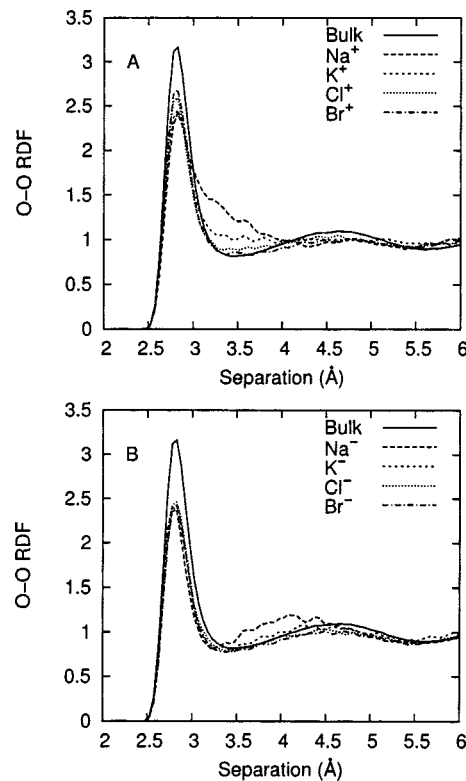


FIG. 4. Oxygen-oxygen RDFs for waters in the first solvation shell. RDFs were computed for water oxygens, including only those pairs where at one of the waters was in the first solvation shell of the ion. (a) The distribution functions about cations and (b) for the anions. In both plots, ''bulk'' refers to O–O RDF from an equivalent neat water simulation.

tion of the first peaks are equivalent, they superpose almost perfectly, which would appear to indicate that the basic solvation mechanism is maintained across a range of particle sizes.

Another measure of the solvent ordering around a solute is the electrostatic potential. By definition, the electrostatic potential is on average constant everywhere in an isotropic solution. However, the presence of a solute breaks the symmetry, and if the waters surrounding a solute are ordered, a net electrostatic potential can be induced, even when the solute makes no electrostatic interactions of its own. When we computed the electrostatic potential at the center of the neutral particles using Eq. (2), we found that the potential was positive for all species. Figure 3 shows the electrostatic potential plotted as a function of the effective radius of the neutral species. These results are qualitatively consistent with those obtained by Ashbaugh.[47] It has been argued that the electrostatic potential at the neutral particle ought to make a roughly linear contribution to the charging free energy for the ion.[31,47] This would amount to a difference of $\approx 10$ kcal/mol between the solvation free energies of otherwise equivalent anions and cations, which is similar to the difference in solvation free energies for $K^+$ and $Cl^-$ computed previously.[11] Figure 3 also compares the electrostatic potentials computed for ions with and without explicit polarizability. The curves differ significantly, in that the potential is initially smaller for the polarizable species but drops more slowly at the particles get bigger. This is interesting, because the water oxygen RDFs appear to be independent of the presence of polarizability on the ion. The effect is likely due to subtle adjustments in the hydrogen packing, which are not readily visible in the ion-oxygen RDFs.

**B. Solvent structure around the first solvation shell**

Because of the strong interactions between the ion and the immediately surrounding water, one can effectively con-

sider the first solvation shell to be a part of the ion and examine the solvation of the whole ion-water complex. This is analogous to the logic behind quasichemical calculations of ion solvation.[45,46,48–51] In this case, we ask the question, how do the water-water interactions made by the waters immediately surrounding an ion depend on the ion's charge and size?

We define the first solvation shell geometrically as all the waters with oxygens within the effective radius of the ion, as listed in Table II. It should be noted that other definitions are also reasonable; for example, when using quasichemical theory the coordination number and first solvation shell are defined thermodynamically.[15]

In order to directly examine the solvent structure about the waters in the first solvation shell, we computed oxygen-oxygen RDFs which included only pairs of oxygens where at least one water molecule was in the first shell. The results are shown in Fig. 4. Figure 4(a) contains the RDFs for the first shells around cations, while Fig. 4(b) shows the same for the anions. For comparison purposes, the equivalent O–O RDF from a neat water solution is included in both plots.

In analyzing Fig. 4, we begin with the assumption that the bulk water RDF represents the minimum free energy distribution. It then follows that any uncompensated perturbation to that distribution is thermodynamically unfavorable. In Fig. 4(a), all of the cations diminish the height of the first peak to roughly the same degree, with the larger ions having a slightly lesser effect. Moreover, the smaller ions, especially

024506-6     Alan Grossfield

J. Chem. Phys. **122**, 024506 (2005)

TABLE V. Average number of water-water hydrogen bonds formed by waters in the first solvation shell around the ions. "Intra" describes hydrogen bonds between two waters in the first solvation shell, while "inter" counts hydrogen bonds to waters outside the first shell. The statistical uncertainty in these values is between 0.005 and 0.01.

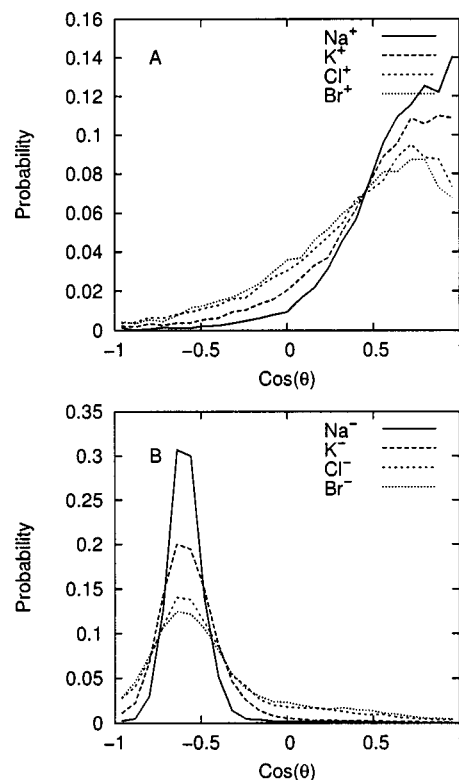| Ion | Positive | | | Negative | | |
|---|---|---|---|---|---|---|
| | Total | Intra | Inter | Total | Intra | Inter |
| Na | 4.17 | 1.58 | 2.59 | 4.18 | 1.56 | 2.62 |
| K | 4.19 | 1.80 | 2.39 | 4.19 | 1.75 | 2.43 |
| Cl | 4.17 | 2.00 | 2.17 | 4.17 | 2.00 | 2.16 |
| Br | 4.12 | 1.97 | 2.15 | 4.22 | 2.06 | 2.16 |



FIG. 5. Probability distribution for the cosine of the angle between the permanent dipole moment of waters in the first solvation shell and the ion-oxygen vector. (a) The distribution functions for the cations and (b) for the anions.

$Na^+$, eliminate the first minimum. The reduction in the first peak is due to volume excluded by the ion, while the diminished minimum indicates that while the first shell waters do have other waters packed around them, they are not part of the typical water-hydrogen bonding network. The differences from the bulk water RDF decrease with increasing effective ionic radius, implying that as the ion-water interactions grow weaker, the water-water interactions become more dominant. This tradeoff between optimizing ion-water and water-water interactions indicates a degree of frustration in the solvation of small cations.

By contrast, the RDFs for the anions, shown in Fig. 4(b), are very similar to the bulk water curve, aside from the fact that the height of the first peak is diminished. With the exception of the smallest anion $Na^-$, the first minimum and long range solvent structure are virtually identical to that for bulk water. This indicates that the presence of the anions does not disrupt the waters' hydrogen bonding network the way cations do.

This dependence on the charge sign is not reflected in the number of hydrogen bonds made by waters in the first solvation shell. As shown in Table V, the total number of hydrogen bonds per water molecule is almost independent of the ionic charge and size. There is a slight shift from hydrogen bonds to bulk waters to hydrogen bonding within the first solvation shell as the ions get larger. Moreover, the increase in intrashell hydrogen bonding is more pronounced for the anions. These trends, while small, do appear to be statistically significant; using Monte Carlo bootstrap error analysis, we estimate that the statistical uncertainties in Table V range from 0.005 to 0.01.

In order to characterize the structure of the first solvation shell in greater detail, we examined the angles between the waters and the ion. Specifically, we computed the probability distribution for the cosine of the angle between the oxygen-ion vector and the permanent dipole moment of the water. The permanent dipole moment of the water is essentially parallel to the bisector of the H–O–H angle; there are small deviations due to fluctuations in the O–H bond lengths. We use the cosine rather than the angle itself because the cosine would have a uniform distribution in the absence of any interactions.

The results are shown in Fig. 5. Figure 5(a) shows the distributions for the cations. The most probable water orientation around the smaller cations is around $\cos(\theta)=1$, corre-

sponding to a structure with the oxygen pointing directly at the ion. However, the distributions are broad, and even for $Na^+$ all orientations are seen. As the ions get bigger, the distribution becomes broader, and the maximum moves away from the parallel orientation; $Cl^+$ and $Br^+$ have maxima around $\cos(\theta)=0.75$ or $\theta \approx 40°$.

It is interesting to note that the probability distributions for all four cations intersect at $\cos(\theta)=0.45$ or about 65°. One could speculate that the angle distributions are composed of two distinct basins of attraction, where one is dominated by ion-water interactions and the other by water-water interactions. If the relative probability of orienting a water molecule with an angle of 65° was the same in both basins, one would expect to see the probability of this angle remain constant even as the ions became larger and the relative importance of ion-water and water-water interactions shifted.

The distribution functions for the anions, shown in Fig. 5(b), are quite different. For all four elements, the distributions are strongly peaked around $\cos(\theta)=-0.6$ corresponding to $\theta \approx 125°$. The complement of this angle, 55°, is almost exactly half of the H–O–H angle, indicating that water primarily points one hydrogen toward the anion. The peaks are broader for the larger anions, but their location does not shift.

The qualitative difference between water structure around cations and anions is indicative of the competition between making strong electrostatic interactions with the ion and maintaining favorable water-water interactions. In the case of the cation, these goals appear to be at odds, with the result that the as the ions grow larger, the distribution shifts

**Downloaded 28 Dec 2004 to 129.34.20.23. Redistribution subject to AIP license or copyright, see http://jcp.aip.org/jcp/copyright.jsp**

TABLE VI. Lifetimes for ion coordination. The autocorrelation function for the instantaneous coordination number for the ions was fit to a sum of two exponentials [see Eq. (4)]. The decay times $\tau_1$ and $\tau_2$ are in picoseconds.

| Ion | Positive | | | | Negative | | | |
| --- | --- | --- | --- | --- | --- | --- | --- | --- |
| | $w_1$ | $\tau_1$ | $w_2$ | $\tau_2$ | $w_1$ | $\tau_1$ | $w_2$ | $\tau_2$ |
| Na | 0.5 | 1.8 | 0.5 | 0.1 | 0.5 | 1.6 | 0.5 | 0.3 |
| K | 0.5 | 0.8 | 0.5 | 0.1 | 0.5 | 0.5 | 0.5 | 0.1 |
| Cl | 0.5 | 0.9 | 0.5 | 0.1 | 0.3 | 1.8 | 0.7 | 0.1 |
| Br | 0.6 | 0.9 | 0.4 | 0.1 | 0.2 | 1.9 | 0.8 | 0.1 |

away from the conformation which optimizes ion-water electrostatics. By contrast, the anion distribution remains centered around the same basic orientation for all of the elements. The weaker electrostatic interactions made by larger ions result in broadening the distribution, but there is no evidence of a competing alternative conformation.

Given the strong electrostatic field surrounding an ion, it is interesting to note that angle probability distribution functions computed using the total dipole moment vector, where the effects of polarization are included, are very similar to those using the permanent dipole (data not shown). The only exception is Na$^-$, where the peak shifts to $\cos(\theta)=0.72$ or $\theta \approx 44°$. However, this does not mean that the ionic electric field completely dominates the water's interactions. For the rest of the ions considered, the angle between the induced dipole on the water and the ion-O vector follows roughly the same distribution as the permanent dipole, and even in the case of Na$^-$ the induced dipole does not typically point directly at the ion.

Furthermore, these electric fields are not as a rule larger in magnitude than those seen in bulk water if one uses the magnitude of the total dipole moment per molecule as the metric. With the AMOEBA water model, bulk water has an average dipole moment of 2.77 D under the conditions simulated here. Waters in the first solvation shell around all of the cations had a slightly smaller dipole moment around 2.72 D. Similar behavior was seen for waters around Cl$^-$ and Br$^-$, where the average dipole moment was 2.74 D. Only the smaller anions caused the overall dipole moment to increase, K$^-$ with 2.81 D and Na$^-$ with 3.11 D.

We also examined the kinetics of waters in the first solvation shell. Specifically, we examined the fluctuations in the coordination numbers for different ionic species. As described in Sec. II, we computed the autocorrelation function for the coordination number and fit it to a sum of two exponentials. The results are shown in Table VI.

In general, there is a fast component to the decay with a time constant $\tau_2$ of 0.1 ps, which accounts for roughly half of the decay, and a slower phase with a time constant $\tau_1$ around 1 ps, which accounts for the rest. However, there is significant variation which is not easily explained by simple trends in size or charge. For Na and K, the behavior is mostly independent of the ionic charge, while for the larger ions the cations and anions behave differently. Cl$^-$ and Br$^-$ have longer $\tau_1$ values than the equivalent cations (roughly 2 ps instead of 1 ps). However, the slow component accounts for

less of the overall decay, where the other ions weight the two components roughly equally.

Physically, we interpret $\tau_1$ to be the time scale for rearrangement of the first solvation shell, while $\tau_2$ most likely represents an artifactual "flickering" as water molecules repeatedly move outside the ion's effective radius without actually leaving the general vicinity of the ion. Thus, we interpret the drop in $\tau_1$ from Na to K as indicating that the larger K species bind their first solvation shell less tightly. By contrast, the longer $\tau_1$ for the larger anions most likely has a different physical origin. We believe it is further indication of the lack of frustration in the first solvation shell's interaction with the bulk.

## IV. DISCUSSION

### A. Charge sign dependence of ion solvation

In a prior paper,[11] we computed the solvation free energies of several ions and observed an interesting phenomenon: the solvation free energy for Cl$^-$ in water was more favorable than that for K$^+$ by roughly 12 kcal/mol and only 5 kcal/mol less favorable than that for Na$^+$. This is in contradiction to what one would expect from a naive application of continuum theory, which would predict that the solvation free energy should increase monotonically with ionic radius, regardless of the sign of the ion's charge. Since the expected behavior was seen in analogous simulations in formamide, we believe this result points to something interesting about the properties of water as a solvent. The primary goal of the present work has been to explain these results by analyzing the effects of ions on water structure as a function of the ions' size and charge.

It has long been common to classify ions into kosmotropes (structure forming) and chaotropes (structure breakers), according to their presumed effects on water structure.[52] However, in the present simulations we see little or no evidence for a global effect of the ions on solvent structure. Rather, the structural properties of waters outside the first solvation shell around the ion are indistinguishable from those seen in simulations of bulk water (data not shown). This is in accordance with recent vibrational spectroscopy experiments, which also reject the notion of ionic effects on global water structure.[53,54]

There are a variety of hypotheses one could attempt to use to explain the surprisingly favorable solvation free energy for Cl$^-$. For example, one could hypothesize that its

effective radius is somehow much smaller that what one would expect based on its crystal radius. However, as shown in Table II, the spacing of waters around chloride follows the expected chemical trend. Moreover, there is no evidence that the ion's charge significantly alters the effective radius. The same is true when the peak heights and well depths are examined in Table IV.

Given the importance of hydrogen bonding in driving water structure, it is reasonable to look at the effect of ions on the number of hydrogen bonds formed by waters in their immediate vicinity. A recent set of calculations using a stylized water model simulated in two dimensions concluded that anions greatly reduce the number of hydrogen bonds made within the first solvation shell, and that the number of intrashell hydrogen bonds increases with ionic radius, regardless of the charge sign.[55] As seen in Table V, the present simulations confirm the latter result; going from the smallest (Na) to largest (Br) ions increases the number of intrashell hydrogen bonds per water molecule by roughly 0.4. However, anions and cations show very similar behavior, which leads us to believe that this is a size effect driven by packing rather than an effect of the ion's charge. Moreover, the total number of hydrogen bonds made by first shell waters remains virtually constant across all of the ions simulated, which makes the observed variation an unlikely candidate to explain the large differences in solvation free energy.

Based on the evidence presented above, we believe that the physical origin of favorable anion solvation is the elimination of frustration in the interactions between the first solvation shell and the bulk water. We base this belief primarily on the evidence from the RDFs computed for these waters (see Fig. 4); while the water-water structure is disrupted around cations, the water-water RDF for the first shell around anions looks almost identical to that for bulk water.

The behavior of water around an uncharged sphere is consistent with this explanation. Because a van der Waals sphere cannot make interactions strong enough to favorably compete with water-water hydrogen bonds, it acts as a probe of what the water "wants" to do, as opposed to what it is "forced" to do by electrostatic interactions with the ion. As shown in Fig. 3, the water induces a positive electrostatic potential at the center of a neutral sphere. While it is clear that adding a charge changes the water structure (see Fig. 2), this does seem to indicate a greater overall compatibility of water structure for anions over cations.

This behavior can also be seen in Fig. 5. Where all of the anions show a single peak in the angle between the water permanent dipole and water around $\theta = 125°$, there is a clear trend in the cation simulations. Waters around $Na^+$ are most likely to orient their dipoles directly at the ion, but this tendency diminishes as the cations get bigger. This is a direct evidence of competition between water-water and water-cation interactions, which appears to be absent with anions. It also points out the naivety of assuming that the water-ion interaction is simply due to charge-dipole interactions. Indeed, a model which does so will mispredict the angle distribution, as well as the resulting water-water packing around the ion.[55] By contrast, angle distributions from all-atom simulations appear very similar to those presented here.[56,57]

## B. Comparison of computational methods

In recent years, a large number of groups have performed simulations exploring the solvation of ions in water, using a variety of techniques ranging from classical force field calculations involving nonpolarizable[20,57–60] and polarizable[11,56,61–71] force fields, to mixed quantum-classical simulations (QM/MM),[15,48,72–74] fully quantum mechanical calculations,[45,46,72,75] and highly simplified models.[30,55,76] Each approach has its advantages and disadvantages. Very simple models tend to make for very inexpensive calculations, so that obtaining sufficient sampling or system size need not be an issue. Moreover, a model with very few terms can make it easy to directly attribute which properties of the simulation are due to which components of the model. However, almost by definition these models involve drastic approximations, and it is not always clear which results are due to the approximations as opposed to the features of the system modeled.

At the other end of the spectrum are fully quantum mechanical calculations. In principle, these methods represent the system with great fidelity. However, they are very expensive computationally, with the result that the systems must be quite small and the sampling very limited; for example, Heuft and Meijer recently used quantum molecular dynamics to simulate a system of 64 waters and one anion for a total of 17 ps.[75] Similarly, Rempe and Pratt simulated $Na^+$ solvated by 32 water molecules for 12 ps.[45] Such simulations typically use small basis sets and either density functional theory or Hartree-Fock theory, both of which neglect attractive dispersion interactions. Still, it is clear that some phenomena, such as solvation of the proton in water, are primarily quantum mechanical in nature and cannot be captured easily without using *ab initio* methods.

Purely classical calculations and QM/MM simulations fall somewhere in between these two extremes, both in terms of expense and accuracy. If one is to use a classical force field, several groups have demonstrated the importance of including explicit electronic polarization in order to accurately describe ionic solvation, especially anions and ions near interfaces, to obtain quantitative accuracy.[11,56,63,67,77,78] However, other groups have shown that it is possible to obtain qualitatively interesting results while only including polarization implicitly.[58]

QM/MM simulations clearly capture electronic polarization at least in the quantum mechanical part of the simulation, and in principle everywhere if a polarizable force field is used for the molecular mechanics part, and while they are significantly more expensive than the equivalent classical calculation, they are efficient enough to allow reasonable system sizes and sampling times. However, like the purely quantum mechanical calculations, they typically use theories which do not contain dispersion interactions. The interface with classical models requires that these interactions be included using empirical potentials.[74,79,80] In principle, this could introduce significant uncertainty into the calculation; in practice, it is not yet clear how sensitive these simulations are to a specific choice of dispersion parameters.[80,81]

Quasichemical theory provides another framework for combining *ab initio* and classical methods.[49] In this ap-

proach, a superion consisting of the ion and a number of inner-shell water molecules are modeled using quantum mechanical methods in gas phase, then transferred into bulk solution using either continuum electrostatics or molecular modeling techniques. Because only a single *ab initio* optimization is performed for each superion cluster (although several cluster sizes must be considered to determine the optimal coordination number), the remainder of the calculation is performed classically, which reduces their computational cost. While this theory correctly accounts for the statistical mechanics of ion transfer, its usual implementation neglects packing and dispersion interactions between the superion and the bulk,[46,51,82] which diminishes the quantitative accuracy of the method. The method also assumes that the fluctuations of the first solvation shell are accurately represented by harmonic fluctuations about the gas phase minimum energy structure for each inner shell coordination number. This approach is analogous to the application of the inherent structures formalism to the interpretation of the behavior of bulk liquids.[83] Moreover, as with other QM/MM methods it is not always clear how to model the interactions between the classical and quantum mechanical portions of the system. Still, this technique has been used to produce a number of interesting results, including calculations of ion solvation free energies and coordination numbers,[45,46,48,50,51,84] and it does provide a clear framework from which one can examine ion solvation.

## V. CONCLUSION

We have presented molecular dynamics simulations using a polarizable force field which explains the differences in solvation between cations and anions. Specifically, the waters in the first solvation shell around an anion are able to maintain water-water interactions which greatly resemble those formed in the bulk liquid, while the waters around smaller cations cannot. However, the present simulations have only treated monovalent atomic ions, and it would be interesting to see if this behavior is retained for more complicated ions such as $Ca^{+2}$, $SO_4^{-2}$, or $ClO_4^-$. Similarly, the effects of ions on water structure near macromolecular assemblies, such as nucleic acids, protein, and lipid bilayers, are of both biological and physical interest.

## ACKNOWLEDGMENTS

[1] D. A. Doyle, J. M. Cabrat, R. A. Pfuetzner, A. Kuo, J. M. Gulbis, S. L. Cohen, B. T. Chait, and R. MacKinnon, Science **280**, 69 (1998).

[2] B. Hille, *Ionic Channels of Excitable Membranes* (Sinauer, Sunderland, MA, 1984).

[3] Y. Zhou and R. MacKinnon, Biochemistry **43**, 4978 (2004).

[4] H. Ohtaki and T. Radnai, Chem. Rev. (Washington, D.C.) **93**, 1157 (1993).

[5] H. Ohtaki, Monatsch. Chem. **132**, 1237 (2001).

[6] H. L. Friedman and C. V. Krishnan, in *Water: A Comprehensive Treatise*, edited by F. Franks (Plenum, New York, 1973), Vol. 3, pp. 1–118.

[7] R. A. Marcus and N. Sutin, Biochim. Biophys. Acta **811**, 265 (1985).

[8] C. Kalidas, G. Hefter, and Y. Marcus, Chem. Rev. (Washington, D.C.) **100**, 819 (2000).

[9] R. Schmid, A. M. Miah, and V. N. Sapunov, Phys. Chem. Chem. Phys. **2**, 97 (2000).

[10] M. D. Tissandier, K. A. Cowen, W. Y. Feng, E. Gundlach, M. H. Cohen, A. D. Earhart, J. V. Coe, and T. R. J. Tuttle, J. Phys. Chem. A **102**, 7787 (1998).

[11] A. Grossfield, P. Ren, and J. W. Ponder, J. Am. Chem. Soc. **125**, 15671 (2003).

[12] C.-G. Zhang and D. A. Dixon, J. Phys. Chem. A **105**, 11534 (2001).

[13] C.-G. Zhang and D. A. Dixon, J. Phys. Chem. A **106**, 9737 (2002).

[14] C.-G. Zhang and D. A. Dixon, J. Phys. Chem. A **108**, 2020 (2004).

[15] D. Asthagiri, L. R. Pratt, and H. S. Ashbaugh, J. Chem. Phys. **119**, 2702 (2003).

[16] W. M. Latimer, K. S. Pitzer, and C. M. Slansky, J. Chem. Phys. **7**, 108 (1939).

[17] J. Åqvist, J. Phys. Chem. **94**, 8021 (1990).

[18] A. D. MacKerell, Jr., D. Bashford, M. Bellott *et al.*, J. Phys. Chem. B **102**, 3586 (1998).

[19] B. Roux and S. Berneche, Biophys. J. **82**, 1681 (2002).

[20] M. Patra and M. Karttunen, J. Comput. Chem. **25**, 678 (2004).

[21] D. Feller, E. D. Glendening, D. E. Woon, and M. W. Feyereisen, J. Chem. Phys. **103**, 3526 (1995).

[22] S. S. Xantheas, J. Phys. Chem. **100**, 9703 (1996).

[23] K. Hiraoka, S. Mizuse, and S. Yamabe, J. Phys. Chem. **92**, 3943 (1988).

[24] P. Ren and J. W. Ponder, J. Phys. Chem. B **107**, 5933 (2003).

[25] M. Born, Z. Phys. **1**, 45 (1920).

[26] A. A. Rashin and B. Honig, J. Phys. Chem. **89**, 5588 (1985).

[27] T. Abe, J. Phys. Chem. **90**, 713 (1986).

[28] S. L. Chan and C. Lim, J. Phys. Chem. **98**, 692 (1994).

[29] J. K. Hyun, C. S. Babu, and T. Ichiye, J. Phys. Chem. **99**, 5187 (1995).

[30] M. Boström and B. W. Ninham, J. Phys. Chem. B **108**, 12593 (2004).

[31] G. Hummer, L. R. Pratt, and A. E. Garcia, J. Phys. Chem. **100**, 1206 (1996).

[32] P. Ren and J. W. Ponder, J. Phys. Chem. B (to be published).

[33] P. Ren and J. W. Ponder, J. Comput. Chem. **23**, 1497 (2002).

[34] J. W. Perram, H. G. Petersen, and S. W. De Leeuw, Mol. Phys. **65**, 875 (1988).

[35] T. A. Halgren, J. Am. Chem. Soc. **114**, 7827 (1992).

[36] P. Ren and J. W. Ponder, J. Phys. Chem. B **108**, 13427 (2004).

[37] D. Beeman, J. Comput. Phys. **20**, 130 (1976).

[38] H. J. C. Berendsen, J. P. M. Postma, W. F. van Gunsteren, A. DiNola, and J. R. Haak, J. Chem. Phys. **81**, 3684 (1984).

[39] J. W. Ponder, TINKER: Software Tools for Molecular Design 3.9, http://dasher.wustl.edu/tinker/ (2001).

[40] G. Hummer, L. R. Pratt, and A. E. Garcia, J. Chem. Phys. **107**, 9275 (1997).

[41] F. Figueirido, G. S. Del Buono, and R. M. Levy, J. Chem. Phys. **103**, 6133 (1995).

[42] S. Bogusz, T. E. I. Cheatham, and B. R. Brooks, J. Chem. Phys. **108**, 7070 (1998).

[43] P. H. Hünenberger and J. A. McCammon, Biophys. Chem. **78**, 69 (1999).

[44] W. H. Press, S. A. Teukolsky, W. T. Vetterling, and B. P. Flannery, *Numerical Recipes in C*, 2nd ed. (Cambridge University Press, Cambridge, 1992).

[45] S. B. Rempe and L. R. Pratt, Fluid Phase Equilib. **183**, 121 (2001).

[46] S. B. Rempe, D. Asthagiri, and L. R. Pratt, Phys. Chem. Chem. Phys. **6**, 1966 (2004).

[47] H. S. Ashbaugh, J. Phys. Chem. B **104**, 7235 (2000).

[48] P. Grabowski, D. Riccardi, M. A. Gomez, D. Asthagiri, and L. R. Pratt, J. Phys. Chem. A **106**, 9145 (2002).

[49] M. E. Paulaitis and L. R. Pratt, Adv. Protein Chem. **62**, 282 (2002).

[50] D. Asthagiri, L. R. Pratt, J. D. Kress, and M. A. Gomez, Chem. Phys. Lett. **380**, 530 (2003).

[51] D. Asthagiri, L. R. Pratt, M. E. Paulaitis, and S. B. Rempe, J. Am. Chem. Soc. **126**, 1285 (2004).

[52] K. D. Collins and M. W. Washabaugh, Q. Rev. Biophys. **18**, 323 (1985).

[53] A. W. Omta, M. F. Kropman, S. Woutersen, and H. J. Bakker, Science **301**, 347 (2003).

[54] M. F. Kropman and H. J. Bakker, J. Am. Chem. Soc. **126**, 9135 (2004).

[55] B. Hribar, N. T. Southall, V. Vlachy, and K. A. Dill, J. Am. Chem. Soc. **124**, 12302 (2002).

[56] M. A. Carignano, G. Karlström, and P. Linse, J. Phys. Chem. B **101**, 1142 (1997).

[57] J. N. Sachs, H. I. Petrache, D. M. Zuckerman, and T. B. Woolf, J. Chem. Phys. **118**, 1957 (2003).

[58] J. N. Sachs and T. B. Woolf, J. Am. Chem. Soc. **125**, 8742 (2003).

[59] D. Bhatt, J. Newman, and C. J. Radke, J. Phys. Chem. B **108**, 9077 (2004).

[60] H.-S. Kim, Chem. Phys. **253**, 305 (2000).

[61] P. Jungwirth and D. J. Tobias, J. Phys. Chem. B **104**, 7702 (2000).

[62] P. Jungwirth and D. J. Tobias, J. Phys. Chem. B **105**, 10468 (2001).

[63] P. Jungwirth and D. J. Tobias, J. Phys. Chem. B **106**, 6361 (2002).

[64] P. Jungwirth and D. J. Tobias, J. Phys. Chem. A **106**, 379 (2002).

[65] H. H. Loeffler and B. M. Rode, J. Comput. Chem. **24**, 1232 (2003).

[66] R. Ayala, J. M. Martínez, R. R. Pappalardo, H. Saint-Martín, I. Ortega-Blake, and E. Sánchez Marcos, J. Chem. Phys. **117**, 10512 (2002).

[67] M. Carrillo-Tripp, H. Saint-Martín, and I. Ortega-Blake, J. Chem. Phys. **118**, 7062 (2003).

[68] L. X. Dang and T.-M. Chang, J. Phys. Chem. B **106**, 235 (2002).

[69] L. X. Dang, J. Phys. Chem. B **106**, 10388 (2002).

[70] D. Spångberg and K. Hermansson, J. Chem. Phys. **120**, 4829 (2004).

[71] T. S. Hofer, H. T. Tran, C. F. Schwenk, and B. M. Rode, J. Comput. Chem. **25**, 211 (2004).

[72] J. A. White, E. Schwegler, G. Galli, and F. Gygi, J. Chem. Phys. **13**, 4668 (2000).

[73] A. Tongraar and B. M. Rode, Phys. Chem. Chem. Phys. **5**, 357 (2003).

[74] A. Öhrn and G. Karlström, J. Phys. Chem. B **108**, 8452 (2004).

[75] J. M. Heuft and E. J. Meijer, J. Chem. Phys. **119**, 11778 (2003).

[76] G. Karlström and D. Hagberg, J. Phys. Chem. B **106**, 11585 (2002).

[77] S. J. Stuart and B. J. Berne, J. Phys. Chem. **100**, 11934 (1996).

[78] L. Perera and M. L. Berkowitz, J. Chem. Phys. **96**, 8288 (1992).

[79] H. Liu, M. Elstner, E. Kaxiras, T. Frauenheim, J. Hermans, and W. Yang, Proteins: Struct., Funct., Genet. **44**, 484 (2001).

[80] H. Hu, M. Elstner, and J. Hermans, Proteins: Struct., Funct., Genet. **50**, 451 (2003).

[81] D. Riccardi, G. Li, and Q. Cui, J. Phys. Chem. B **108**, 6467 (2004).

[82] G. Hummer, L. R. Pratt, and A. E. Garcia, J. Phys. Chem. A **41**, 7885 (1998).

[83] F. H. Stillinger and T. A. Weber, Phys. Rev. A **25**, 978 (1982).

[84] D. Asthagiri, L. R. Pratt, J. D. Kress, and M. A. Gomez, Proc. Natl. Acad. Sci. U.S.A. **101**, 7229 (2004).